Analyst

Accepted Manuscript

This article can be cited before page numbers have been issued, to do this please use: E. Lee, H. Jeon, J. Ryu, C. Kang, S. Kim, S. Park and Y. Kwon, *Analyst*, 2020, DOI: 10.1039/D0AN01116A.

ROYAL SOCIETY OF CHEMISTRY

rsc.li/analyst

View Article Online
DOI: 10.1039/D0AN01116A

ARTICLE

Genetically encoded biosensors for the detection of rapamycin: toward the screening of agonists and antagonists

Received 00th January 20xx,
Accepted 00th January 20xx

DOI: 10.1039/x0xx00000x

Euiyeon Lee,[a] Hyunjin Jeon,[a,b] Jeahee Ryu,[a] Chungwon Kang,[a] Soyoun Kim,[a] Seungil Park,[a] and Youngeun Kwon*[a]

Biosensors are valuable tools for the rapid screening of biological targets with high sensitivity and specificity. It is important to screen biological events in their native context for pharmacological and toxicological applications. However, *in vitro* biosensors often require purified probes and targets for screening, thus providing limited information on targets' biological activities in their native environment. To address this issue, we developed a cell-based sensing system that could detect a biologically active small molecule, rapamycin (Rapa). We designed a reporter system based on fluorescence translocation by signal peptide reconstitution. Herein, the signal peptides are activated by conditional protein splicing without the need for refolding into a functional tertiary structure, thus eliminating false positives and negatives due to mere binding or misfolding. The developed biosensor demonstrated excellent sensitivity with a limit of detection of 0.1 nM, and it was able to screen the agonist and antagonist of Rapa. The developed cell-based sensing system could contribute improving the screening system aimed to identify the natural mimetics of Rapa and potential drug candidates.

1. Introduction

Rapamycin (Rapa) is a macrocyclic lactone (macrolide) derived from the bacterium *Streptomyces hygroscopicus*, and it was first discovered in a soil sample from Easter Island, an island also known as Rapa Nui.[1] Rapa exerts potent immunosuppressive activity and has been used as an immunosuppressant in organ transplantation since 1999.[2] It was also approved as an anti-cancer drug as it showed anti-proliferative activity against several cancer types, including cervical, breast, lung, and colon cancers.[3] Furthermore, recent experimental studies conducted using yeast, fruit flies, and mice found that Rapa could effectively extend their lifespan.[4, 5] Despite the various drug effects of Rapa, there are some limitations of the long-term use of Rapa as it reportedly causes adverse effects such as wound complications and ulcers.[6] In addition, the poor solubility and pharmacokinetics of Rapa triggered the development of Rapa analogs, such as temsirolimus and everolimus.[1]

To screen for agonists and antagonists of drugs, *in vitro* assays are often performed on a microtiter plate.[7, 8] These assays are simple and produce consistent results but do not guarantee high biological relevance as they are performed in dissimilar environments.[9, 10] Whole-cell-based sensing systems are a better alternative to *in vitro* assays because they reflect biological systems more accurately.

During the past decades, the assay capability of *in vitro* biosensors has greatly improved.[11-14] In particular, recombinant protein biosensors have become a popular tool for drug target identification, which combine the specificity provided by ligand-binding proteins and the sensitivity provided by fluorescence and/or luminescence signals.[15-18] These biosensors often utilize optical reporters based on bimolecular fluorescence/luminescence complementation (BiFC/BiLC) or Förster resonance energy transfer (FRET). Although these reporting systems are useful, there are some drawbacks, such as high background signals and false-negatives due to tricky refolding conditions.

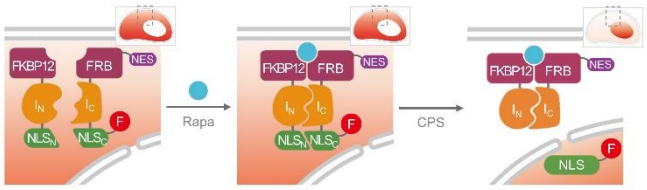

Scheme 1 A schematic of fluorescence translocation in sensor cells via conditional protein splicing (CPS). The split intein-mediated CPS reaction was used to activate the signal peptide. Rapamycin (Rapa) induces the heterodimerization of FKBP12 and FRB to trigger CPS. The split signal peptides are reconstituted *via* a stable amide bond with restored activity. The fluorescent reporter is translocated by the activated signal peptide and reports the presence of the target molecule.

[a] Department of Biomedical Engineering (BK21 plus), Dongguk University, Seoul 04620, Korea
[b] Gencurix Inc. 3F, 242 Digital-ro, Guro-gu, Seoul 08394, Korea
Electronic Supplementary Information (ESI) available: [details of any supplementary information available should be included here]. See DOI: 10.1039/x0xx00000x

View Article Online
DOI: 10.1039/D0AN01158A

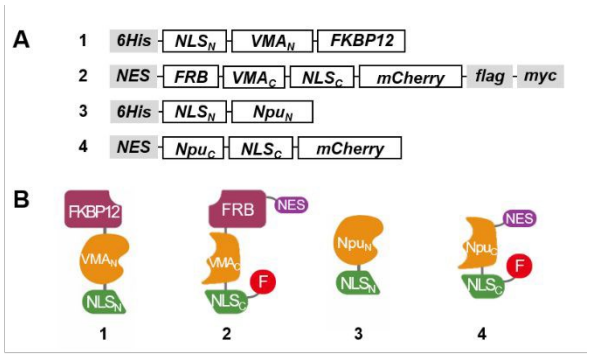

Fig. 1 Fusion proteins used in this study. (A) Domain architecture of the DNA constructs of the fusion proteins containing N- or C-intein fragments. (B) Schematic illustration of fusion proteins **1–4**.

As an alternative to current approaches, we recently reported a live cell-based sensing system which was used to screen biologically active signaling molecules, such as Ca^{2+} and stress hormones. These live cell-based sensors could provide functional information about targets as well as analytical information and allowed for the screening of functional analogs (agonists) while differentiating them from structural analogs.[19] The developed cell-based sensors utilized the fluorescence translocation reporting system, which is based on the activation of signal peptides by conditional protein splicing (CPS). Unlike split proteins, signal peptides do not require folding into a functional tertiary structure to regain their activity nor can they be activated via the simple binding of the two split fragments. As the use of signal peptides can minimize the false-positive or -negative signals originating from protein–protein interactions or the misfolding of reporter proteins, this approach offers a method to overcome the limitations of FRET and BiFC-based detection.[20]

In this study, we focused on the development of a live-cell biosensor for the detection of Rapa and its agonist. The key to our approach is the activation of signal peptides and the consequent fluorescence translocation mediated by the CPS reaction with the target molecule Rapa as an activation switch (Scheme 1). We used the heterodimerization of FK506-binding protein (FKBP12) and FKBP-rapamycin binding domain (FRB) for the detection of Rapa and its agonist. Split VMA inteins were used for the CPS system as they do not have sufficiently high binding affinity to each other, thus requiring induced dimerization to perform protein splicing reactions.[21-23] The developed sensors were tested for the detection of Rapa as well as the screening of the agonist and antagonist of Rapa.

2. Experimental

2.1 General procedures

DNA primers were purchased from Mbiotech (Hanam, Korea). Restriction enzymes were purchased from Elpis Biotech (Daejeon, Korea) and New England Biolabs (Ipswich, MA). General cell culture reagents were purchased from Invitrogen Life Technologies (Carlsbad, CA) and Welgene (Daegu, Korea). SDS-PAGE and Western blot analyses were performed according to standard protocols. Confocal fluorescence images were obtained using an Eclipse Ti confocal microscope (Nikon Instruments, Tokyo, Japan) with excitation wavelengths of 358, 488, and 594 nm and their corresponding emission filters. The fluorescence intensity was measured using the Nikon NIS-Element BR 4.60 software.

2.2 Molecular biology and construct design

DNA cloning was performed according to standard protocols. All constructed plasmids were confirmed by DNA sequencing and amplified using the *E. coli* strain DH5α. The cDNA encoding the N-terminal domain of the *Saccharomyces cerevisiae* VMA intein (VMA_N) in pET28a was modified by introducing the cDNA encoding His6 tag and the N-terminal fragment of the nuclear localization signal (NLS_N; KRPAATKKA) into the N-terminus between NcoI and NheI sites, and the cDNA encoding FK506-binding protein (FKBP12) was inserted into the C-terminus between SalI and XhoI to create construct **1** (NLS_N-VMA_N-FKBP). The cDNA encoding the C-terminal domain of the VMA intein (VMA_C) in pET28a was modified by introducing the cDNA encoding the C-terminal fragment of NLS (NLS_C; GQAKKKKLD) and mCherry into the C-terminus between NheI and XhoI sites. In addition, the resulting construct was modified by inserting the cDNA encoding the nuclear export signal (NES; NELALKLAGLDINKT) and FKBP-rapamycin binding domain (FRB) into the N-terminus between NcoI and NdeI sites to create construct **2** (FRB-VMA_C-NLS_C-mCherry**)**. The cDNA encoding *Nostoc punctiforme* DnaE N-intein (Npu_N) in pBI-CMV1 was modified by introducing the cDNA encoding His6 tag and NLS_N into the N-terminus between MluI and NotI sites to create construct **3**. The cDNA encoding Npu DnaE C-intein (Npu_C) in pBI-CMV1 was modified by introducing the cDNA encoding NLS_C and mCherry to the C-terminus between ApaI and XbaI sites. The resulting construct was modified by inserting the cDNA encoding NES into the N-terminus between AgeI and ApaI sites to create construct **4**.

2.3 Cell culture and transfections

HeLa and HEK293T (ATCC, Manassas, VA) cells were maintained in Dulbecco's modified Eagle's medium (DMEM; Welgene, Daegu, Korea) supplemented with 10% (v/v) fetal bovine serum (FBS) gold (Welgene, Daegu, Korea) and 1% (v/v) antibiotics (100 μg/mL streptomycin, 20 U/mL penicillin). All cells were maintained at 37°C in a humidified incubator with 5% CO_2. To observe fluorescence translocation in drug-stimulated cells, HeLa and HEK293T cells were seeded on 35-mm confocal dishes (5×10^4 cells) for 24 h before experimentation. After 1 day of cultivation to promote cell attachment and spreading, transfection was performed using Lipofectamine 2000 according to the manufacturer's protocol (Invitrogen Life Technologies, Carlsbad, CA).

2.4 Live-cell imaging for Rapa detection

For live-cell imaging, HeLa and HEK293T cells were separately grown in 35-mm confocal dishes. The cells were transiently transfected using a pIRES vector encoding fusion proteins **1** and

View Article Online
DOI: 10.1039/D0AN01116A

2. Protein expression was allowed to proceed at 37°C for 24 h, and the cells were treated with 10 nM Rapa at 30°C. The cells were washed with PBS, and their nuclei were stained with Syto9 (3 μM) or Hoechst (8 μM). Then, the fluorescence images were obtained to monitor the Rapa-mediated fluorescence translocation. At least 3 experiments were performed and ~30 cells were analyzed in each experiment.

concentrations of FK506 (0.1, 1, 10, 100, 1000, and 10000 nM) in the presence of 1 nM Rapa for 2 h at 30°C. The fluorescence images were obtained to monitor the fluorescence translocation. At least 30 cells were analyzed in each experiment. The K_i was calculated using the equation of Cheng and Prusoff[24] which is shown in Eq.(1):

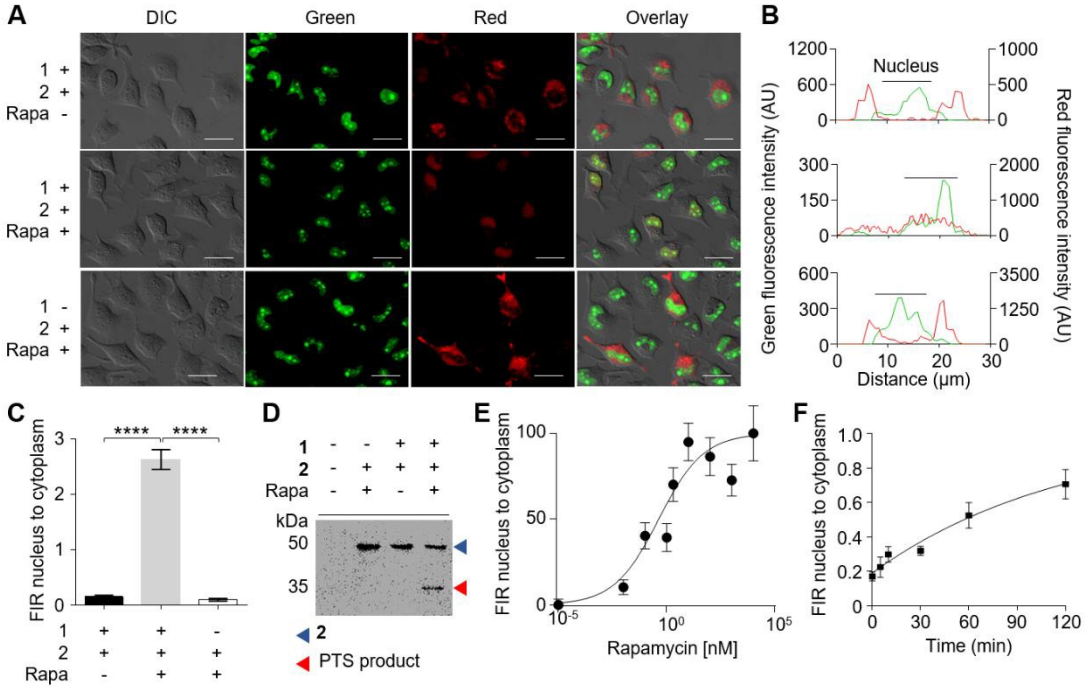

Fig. 2 Detection of rapamycin (Rapa) using sensor cells based on fluorescence translocation. (A) Sensor cells co-expressing proteins **1** and **2** showed red fluorescence in the cytoplasm before Rapa stimulation (row 1). The red fluorescence signal was translocated to the nucleus when the sensor cells were challenged with Rapa (row 2). The control cells expressing only protein 2 did not respond to Rapa stimulation (row 3). The nucleus was stained with Syto9 (green). Scale bar = 25 μm. (B) The location of the red fluorescence signal was examined. Green fluorescence indicates the location of the nucleus. (C) The nucleus-to-cytoplasm fluorescence intensity ratio (FIR) was quantitatively analyzed using at least 30 cells. Statistical analysis was performed using one-way ANOVA with Tukey's multiple comparison test (****$p < 0.0001$). (D) Western blot analysis revealed the formation of PTS products 2 h after stimulation. (E) The dose–response curve demonstrated increased fluorescence translocation with increasing Rapa concentration. The LOD was 0.1 nM, and the EC_{50} was 0.4 nM. The LOD was determined to be three times the standard deviation of negative control. (F) The time-response curve demonstrated increased fluorescence translocation over time with near saturation after 1 h.

2.5 Live-cell imaging for screening the agonist and antagonist of Rapa

For live-cell imaging, HeLa and HEK293T cells were separately grown in 35-mm confocal dishes. The cells were transiently transfected using a pIRES vector encoding fusion proteins 1 and 2. Protein expression was allowed to proceed at 37°C for 24 h, and the cells were individually treated with 100 nM Rapa, temsirolimus (CCI-779), or tacrolimus (FK506) for 2 h at 30°C. The fluorescence images were obtained to monitor the agonist and antagonist of Rapa-mediated fluorescence translocation. At least 3 experiments were performed and ~30 cells were analyzed in each experiment.

2.6 Competitive inhibition assay using FK506

To determine the apparent inhibition constant (K_i) of FK506-mediated inhibition of fluorescence signal translocation in live cells, the sensor cells were treated with the indicated

$$K_i = \frac{IC_{50}}{1 + \frac{[Rapa]}{K_d}} \qquad (1)$$

2.7 Western blotting

For Western blot analysis, HeLa cells were grown in 100-mm dishes. The cells were stimulated individually with Rapa, CCI-779, or FK506 and then collected and lysed for 1 h on ice in 200 μL of 1% SDS in RIPA buffer containing a protease inhibitor cocktail. Cell lysates were mixed with 0.2 volumes of 5× SDS-PAGE loading buffer and analyzed by SDS-PAGE. The formation of the splicing product was monitored by Western blotting using anti-mCherry or anti-myc antibody.

2.8 Statistics

All data are presented as mean ± SEM. Data were analysed and

View Article Online
DOI: 10.1039/D0AN01116A

figures were drawn using GraphPad Prism 7.0 (San Diego, CA). *P*-value <0.05 was considered significant.

Results and discussion

3.1 Design of a genetically encoded biosensor for the detection of Rapa

splicing reactions. Then, we introduced split fragments of signal peptides (NLS_N and NLS_C) and an mCherry fluorescent protein as exteins of VMA inteins to obtain NLS_N-VMA_N-FKBP **1** and FRB-VMA_C-NLS_C-mCherry **2** (Fig. 1). The key to our approach is that Rapa, which is the target, induces the heterodimerization of FKBP12 and FRB as well as the binding of the split VMA inteins to trigger the CPS reaction. The signal peptide is reconstituted via the CPS reaction to generate a detectable

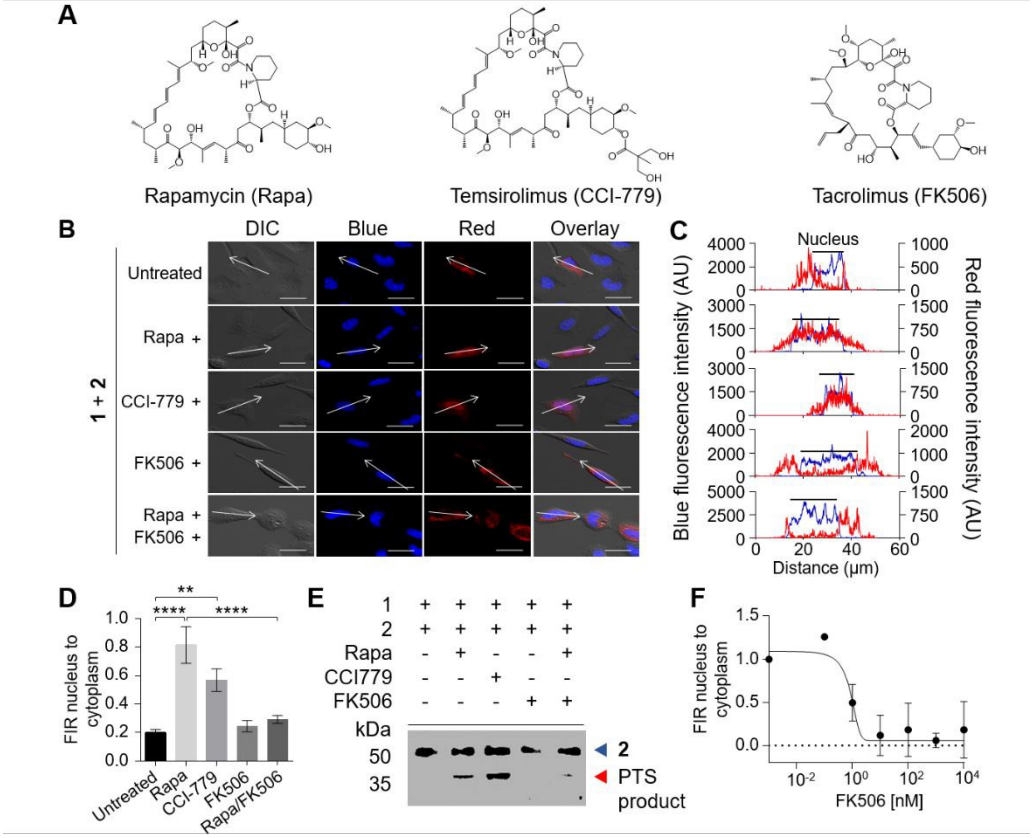

Fig. 3 Screening of the agonist and antagonist of rapamycin (Rapa) using sensor cells. (A) The structures of the Rapa, temsirolimus (CCI-779), and tacrolimus (FK506) are shown. Rapa binds simultaneously to FKBP12 and FRB and controls various cellular processes. CCI-779 is a functional analog (agonist) of Rapa. FK506 is a structural analog of Rapa without FRB-binding affinity. (B) Sensor cells expressing fusion proteins **1** and **2** showed red fluorescence in the cytoplasm prior to stimulation (rows 1–5). The sensor cells responded to Rapa and CCI-779 treatments, as demonstrated by the translocation of the fluorescence signal to the nucleus (rows 2 and 3, respectively). The cells discriminated against the structural analog FK506, and the fluorescence signal was largely localized in the cytoplasm (row 4). FK506 inhibited Rapa-mediated signalling in the sensor cells (row 5). (C) The location of the red fluorescence signal was examined. Blue fluorescence indicates the location of the nucleus. (D) The nucleus-to-cytoplasm fluorescence intensity ratio (FIR) was quantitatively analyzed using at least 30 cells. Statistical analysis was performed using one-way ANOVA with Tukey's multiple comparison test (**p < 0.01, ****p < 0.0001). (E) Western blot analysis revealed the formation of PTS products 2 h after stimulation. PTS product formation was not observed in sensor cells treated with FK506. (F) Sensor cells expressing fusion proteins **1** and **2** were treated with the indicated concentrations of FK506 in the presence of Rapa. The K_i of FK506-mediated inhibition of Rapa-induced fluorescence signal translocation was determined (K_i = 1 nM).

We designed a sensing system to detect Rapa based on the activation of signal peptides in living cells. To construct a Rapa-sensing system, we designed a CPS system exploiting a well-studied pair of *Saccharomyces cerevisiae* split VMA inteins. Since the split VMA inteins (VMA_N and VMA_C) have little or no affinity for each other, the protein trans-splicing (PTS) reaction can be activated by the induced dimerization of the two split fragments.

It is well-known that FKBP12 can be activated and binds to the FRB in the presence of Rapa.[25] We configured the CPS system using a strategy reported by Mootz and Muir.[21] First, we designed two fusion proteins (VMA_N-FKBP and FRB-VMA_C) that heterodimerize in the presence of Rapa and carry out protein optical signal, i.e., the translocation of a fluorophore-conjugated signal peptide (Scheme 1).

3.2 Construction of genetically encoded sensor cells

The domain architectures of the gene construct and fusion proteins are shown in Figure 1. Fusion proteins **1** and **2** each contain one half of the split VMA inteins. The split signal peptides were used as exteins; the target recognition units FKBP12 and FRB were introduced to the other ends of VMA_N and VMA_C inteins, respectively, and the red fluorescent mCherry protein was attached to the C-terminus of the VMA_C-containing fusion protein as an optical reporter. The NLS peptide (KRPAATKKAGQAKKKKLD) was modified by inserting a

View Article Online
DOI: 10.1039/D0AN01116A

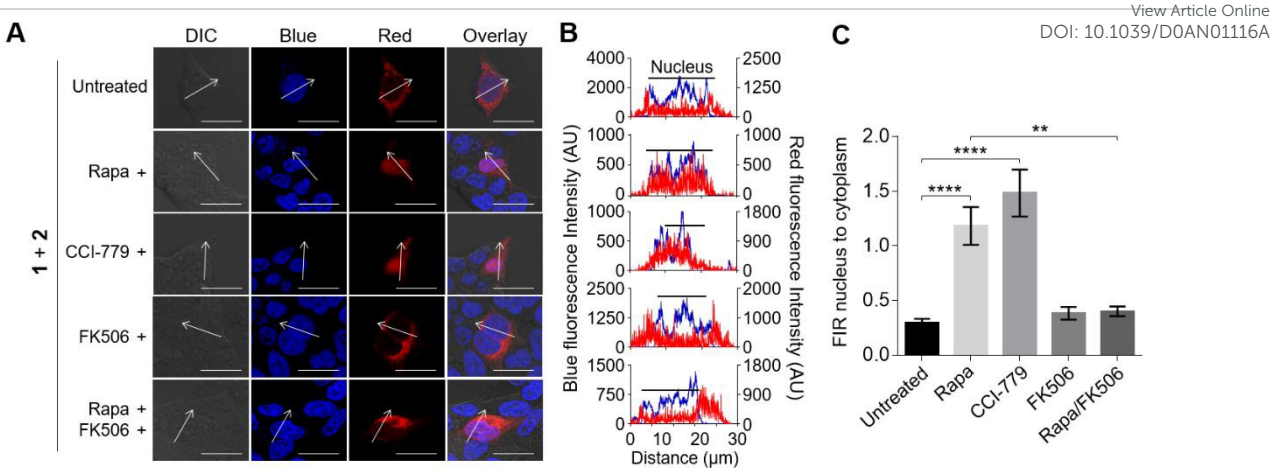

Fig. 4 HEK293T sensor cells for rapamycin (Rapa) and analog screening. (A) HEK293T cells were transfected to express fusion proteins 1 and 2 to generate sensor cells. The sensor cells showed red fluorescence in the cytoplasm before stimulation (rows 1–5). The sensor cells responded to Rapa and CCI-779 treatments by showing the translocation of the fluorescence signal to the nucleus (rows 2 and 3, respectively). The sensor cells discriminated against the structural analog FK506, and no apparent fluorescence translocation was observed (row 4). FK506 inhibited Rapa-mediated translocation in the sensor cells (row 5). (B) The location of the red fluorescence signal was examined. Blue fluorescence indicates the location of the nucleus. (C) The location of the red fluorescence signal was examined. Blue fluorescence indicates the location of the nucleus. (D) The nucleus-to-cytoplasm fluorescence intensity ratio (FIR) was quantitatively analyzed using at least 30 cells. Statistical analysis was performed using one-way ANOVA with Tukey's multiple comparison test (**p < 0.01, ****p < 0.0001).

short linker, SCFNAS, to ensure PTS activity, thus providing the KRPAATKKASCFNASGQAKKKKLD as a recombinant NLS (rNLS) sequence.[26-28] We previously demonstrated that the extra amino acids in the signal peptide did not hinder the activity of rNLS.[19] rNLS was split at position 10 to generate two inactive split peptides, NLS_N (KRPAATKKAS) and NLS_C (CFNASGQAKKKKLD), and these peptides were used as N- and C-exteins, respectively. A nuclear export signal (NES; NELALKLAGLDINKT) that originated from PKI-a was incorporated into the N-terminus of VMA_C to ensure that the red fluorescence signal is located in the cytoplasm initially. In addition, myc and flag tags were introduced to the VMA_C-containing fusion protein for Western blot analysis. Constructs **1** and **2** were inserted into a pIRES vector containing two constitutive promoters and transiently introduced to HeLa cells. Among the two multiple cloning sites, we chose the one with less active expression for construct **2** to minimize the background signal. Before the CPS-based sensing of Rapa, the generation of signal peptides by PTS and consequent fluorescence translocation were validated using a spontaneously reacting pair of split inteins (Npu DnaE). The results confirmed the *in vivo* reconstitution of active signal peptides via PTS and the subsequent translocation of fluorescent cargos (Fig. S1).

3.3 Detection of Rapa using genetically encoded sensor cells

To evaluate the performance of sensor cells, HeLa cells expressing both constructs **1** and **2** were treated with Rapa (10 nM, 2 h). The live sensor cells were used without fixation to monitor the location of the red fluorescence signal by confocal fluorescence microscopy before and after the Rapa treatment. The red fluorescence signal in sensor cells was primarily localized in the cytoplasm without the Rapa treatment (Fig. 2A, row 1) and then translocated to the nucleus following the Rapa treatment (Fig. 2A, row 2). Cells transfected with only construct **2** did not respond to Rapa stimulation (Fig. 2A, row 3), suggesting that the observed fluorescence translocation in sensor cells may be attributed to split intein-mediated PTS. Western blot analysis confirmed the covalent conjugation of signal peptides, i.e., the formation of PTS products (Fig. 2D). The average nucleus-to-cytoplasm fluorescence intensity ratio (FIR, the ratio of the red fluorescence signal in the nucleus to that in the cytoplasm) was quantitatively analyzed before and after Rapa stimulation and showed that approximately 80% of the fluorescence signal translocated to the nucleus in the presence of the target (Fig. 2B and 2C). Taken together, these results showed that the sensor cells could detect and report the presence of Rapa through fluorescence translocation via CPS-mediated reconstitution and activation of signal peptides.

We then monitored the response of sensor cells using varying concentrations of Rapa to determine the limit of detection (LOD) and EC_{50} values. The sensor cells were treated with Rapa concentrations ranging from 0.01 to 10,000 nM (Fig. 2E and Fig. S2) for 2 h. Fluorescence translocation was increased with increasing Rapa concentration up to 10 nM before saturation. The LOD, K_d and EC_{50} were 0.1 nM, 0.08 nM and 0.4 nM, respectively, and these results indicated improved sensitivity compared with previously reported values based on Western blot analysis.[22] FIR was determined for each case, and a similar trend was observed. The maximum FIR of Rapa-stimulated sensor cells was 0.92, and the background signal from non-treated sensor cells was 0.2, resulting the signal-to-noise ratio of 4.6.

Several previously developed cell-based sensor have shown delayed response in comparison with the response of analytical sensors, and the long response time could be a limitation for the practical application of biosensors.[29-33] Therefore, we aimed to build fast-responding sensor cells and tested the response time of the developed sensor cells. The sensor cells were treated with Rapa (100 nM), and the increase in fluorescence translocation

was monitored over time by fluorescence microscopy (Fig. S3). The FIR was determined and plotted at each time point (Fig. 2F). The translocation of the fluorescence signal was detected starting 10 min after Rapa stimulation, and the signal was nearly saturated after 1 h (Fig. S3). These results showed a notable improvement compared with the performance of previously reported translocation sensor cells built using the CAAX tag. The rate-determining step of the sensor cells may be the VMA intein-mediated trans-splicing reaction ($t_{1/2}$ = 60 min).[22]

3.4 Screening agonists and antagonists of Rapa using sensor cells

As the developed sensor cells can screen small molecules based on their biological activities, we exploited the sensor cells to screen the agonist and antagonist of Rapa. The immunosuppressive drug temsirolimus (CCI-779) was chosen as it is a well-known Rapa agonist and an FKBP-binding small molecule, tacrolimus (FK506), was chosen as a Rapa structural analog without FRB-binding affinity (Fig. 3A).[34] The sensor cells were individually treated with CCI-779 and FK506 and monitored by fluorescence microscopy. The sensor cells were able to differentiate the functional analog from the structural analog by reporting the presence of CCI-779 through signal translocation and not responding to the Rapa structural analog FK506 (Fig. 3B). The fluorescence intensity profiles of the nucleus and the cytoplasm were analyzed using the obtained images for each case (Fig. 3C). The FIR was 0.92, 0.58, 0.2, and 0.3 for Rapa-, CCI-779-, FK506-, and Rapa/FK506-treated sensor cells, respectively (Fig. 3D). The antagonistic effects of FK506 was investigated using the sensor cell. The sensor cells were exposed to the increasing concentrations of FK506 in the presence of 1 nM Rapa (Fig. S4). The graph of FIR versus FK506 showed the competitive inhibition with the K_i value was 1 nM (Fig. 3F). The sensor cells allowed the expedited inhibition assay and provided the K_i value, which is comparable to the previously reported K_i of FK506 (4.2 nM). [35] The results showed that our sensor cells could be used for expedited inhibitor screening with increased sensitivity.

Together, these results showed that the developed sensor cells could provide functional information on targets by responding similarly to molecules with the same functions, such as targets and agonists. The sensor cells were also able to discriminate the structurally similar antagonist FK506 with an excellent specificity. The developed sensor cells could be used to screen the functional analogs of targets in a biological environment, thus holding great potential for drug screening applications.

3.5 Generation of sensor cells using different cell lines

In the preparation of genetically encoded sensor cells, the cell type could be an important factor as each cell type has different levels of protein expression and response patterns. Therefore, we investigated whether our approach could be extended to other cell types. Therefore, we decided to evaluate the HEK293T cell line, which is one of the most common cell lines used for research purposes.[36] HEK293T cells were transfected to constitutively express proteins **1** and **2** to obtain sensor cells, and the sensor cells were separately treated with Rapa, CCI-779, and FK506. The fluorescence images showed that the red fluorescence signal was translocated from the cytoplasm to the nucleus when the cells were treated with Rapa or CCI-779, whereas there was no apparent signal translocation in the sensor cells treated with FK506 (Fig. 4). The competitive inhibition of Rapa activity by FK506 was also observed in HEK293T-derived sensor cells (Fig. 4A, row 5). The sensitivity and specificity of HEK293T-derived sensor cells were comparable to those of HeLa-derived sensor cells, suggesting that this approach of constructing genetically encoded sensor cells is applicable to various cell types (Fig. 4B and 4C).

Conclusions

In this study, we developed a live cell biosensor for the detection of Rapa. We designed the reporter system based on the inducible activation of signal peptides, which can transport fluorescent cargos to report the presence of targets. This system is advantageous over other optical reporting systems as it can minimize the false-positive and -negative signals originating from protein–protein interactions or protein misfolding. The developed sensor cells showed excellent performance with increased sensitivity, specificity, and a short response time. The sensor cells were also able to report the presence of the functional analog while differentiating it from the structural analog with different functions. Our results suggest that the cell-based sensing system is applicable for screening the natural mimetics of target molecules, thus allowing for lead identification for drug discovery. Cell-based sensors are emerging tools in the biosensing field, which enable the functional identification of unknown materials with promising biological activities. In particular, live cell biosensors have high potential in several areas, such as pharmacology, toxicology, and environmental research.

Conflicts of interest

There are no conflicts of interest to declare.

Acknowledgements

This work was funded by the MSIP of Korea through the NRF (NRF-2017M3A9C6029322 and NRF-2019R1A2C1088407).

Notes and references

1 J. Li, S. G. Kim and J. *Blenis, Cell metab.*, 2014, **19**, 373-379.
2 S. C. Chueh and B. D. Kahan, *Transpl. Int.*, 2005, **18**, 261-277.
3 S. Vignot, S. Faivre, D. Aguirre and E. Raymond, *Ann. Oncol.*, 2005, **16**, 525-537.
4 R. W. Powers, 3rd, M. Kaeberlein, S. D. Caldwell, B. K. Kennedy and S. Fields, *Genes Dev.*, 2006, **20**, 174-184.
5 D. E. Harrison, R. Strong, Z. D. Sharp, J. F. Nelson, C. M. Astle, K. Flurkey, N. L. Nadon, J. E. Wilkinson, K. Frenkel, C.

S. Carter, M. Pahor, M. A. Javors, E. Fernandez and R. A. Miller, *Nature*, 2009, **460**, 392-395.
6 M. Buchler, S. Caillard, S. Barbier, E. Thervet, O. Toupance, H. Mazouz, B. Hurault de Ligny, Y. Le Meur, A. Thierry, F. Villemain, A. E. Heng, B. Moulin, M. P. Morin, C. Noel and Y. Lebranchu, *Am. J. Transplant.*, 2007, **7**, 2522-2531.
7 M. Ehrbar, R. Schoenmakers, E. H. Christen, M. Fussenegger and W. Weber, *Nat. Mater.*, 2008, **7**, 800-804.
8 M.-S. Yoou, S. Cho and Y. Choi, *BioChip J.*, 2019, **13**, 260-268.
9 E. Michelini, L. Cevenini, L. Mezzanotte, A. Coppa and A. Roda, *Anal Bioanal Chem.*, 2010, **398**, 227-238.
10 J. N. Chan, C. Nislow and A. Emili, *Trends Pharmacol Sci.*, 2010, **31**, 82-88.
11 E. C. Alocilja and S. M. Radke, *Biosens. Bioelectron.*, 2003, **18**, 841-846.
12 A. Rasooly and J. Jacobson, *Biosens. Bioelectron.*, 2006, **21**, 1851-1858.
13 Y. Ding, H.-w. Ai, H. Hoi and R. E. Campbell, *Anal. Chem.*, 2011, **83**, 9687-9693.
14 T. Tamura and I. Hamachi, *ACS Chem. Biol.*, 2014, **9**, 2708-2717.
15 A. Ibraheem and R. E. Campbell, *Curr Opin Chem Biol.*, 2010, **14**, 30-36.
16 Y. Ohba, Y. Fujioka, S. Nakada and M. Tsuda, *Pro Mol Biol Transl Sci.*, 2013, **113**, 313-348.
17 K. Tainaka, R. Sakaguchi, H. Hayashi, S. Nakano, F. F. Liew and T. Morii, *Sensors*, 2010, **10**, 1355-1376.
18 M.-H. Pan, J. Lin, J. L. Prior and D. Piwnica-Worms, *Mol. Cancer Ther.*, 2010, **9**, 2752-2760.
19 H. Jeon, E. Lee, D. Kim, M. Lee, J. Ryu, C. Kang, S. Kim and Y. Kwon, *Anal. Chem.*, 2018, **90**, 9779-9786.
20 S. Daunert, G. Barrett, J. S. Feliciano, R. S. Shetty, S. Shrestha and W. Smith-Spencer, *Chem. Rev.*, 2000, **100**, 2705-2738.
21 H. D. Mootz and T. W. Muir, *J. Am. Chem. Soc.*, 2002, **124**, 9044-9045.
22 H. D. Mootz, E. S. Blum, A. B. Tyszkiewicz and T. W. Muir, *J. Am. Chem. Soc.*, 2003, **125**, 10561-10569.
23 T. Ozawa, T. M. Takeuchi, A. Kaihara, M. Sato and Y. Umezawa, *Anal. Chem.*, 2001, **73**, 5866-5874.
24 Y. Cheng and W. H. Prusoff, *Biochemical pharmacology*, 1973, **22**, 3099-3108.
25 J. Choi, J. Chen, S. L. Schreiber and J. Clardy, *Science*, 1996, **273**, 239.
26 J. P. S. Makkerh, C. Dingwall and R. A. Laskey, *Current Biology*, 1996, **6**, 1025-1027.
27 N. H. Shah, G. P. Dann, M. Vila-Perelló, Z. Liu and T. W. Muir, *J. Am. Chem. Soc.*, 2012, **134**, 11338-11341.
28 N. H. Shah, E. Eryilmaz, D. Cowburn and T. W. Muir, *J. Am. Chem. Soc.*, 2013, **135**, 5839-5847.
29 A. ElMekawy, H. M. Hegab, D. Pant and C. P. Saint, *J. Appl. Microbiol.*, 2018, **124**, 302-313.
30 H. Jeon, M. Lee, W. Jang and Y. Kwon, *BioChip J.*, 2016, **10**, 277-287.
31 H. Jeon, J. H. Jung, Y. Kim, Y. Kwon and S. T. Kim, *Ann Lab Med.*, 2018, **38**, 338-347.
32 J. Ryu, S. Kim, J. Song, D. Kim, N. Keum, W. Jang, H. Bae and Y. Kwon, *Sensors*, 2019, **19**, 3893-3904.
33 D.-H. Kim, S.-H. Paek, D.-Y. Choi, M.-K. Lee, J.-N. Park, H.-M. Cho and S.-H. Paek, *BioChip J.*, 2020, **14**, 2-17.
34 H. H. van Rossum, F. P. Romijn, N. P. Smit, J. W. de Fijter and J. van Pelt, *Biochem. Pharmacol.*, 2009, **77**, 1206-1212.
35 K. E. Luker, M. C. Smith, G. D. Luker, S. T. Gammon, H. Piwnica-Worms and D. Piwnica-Worms, *Proc Natl Acad Sci U S A*, 2004, **101**, 12288-12293.
36 Y.-C. Lin, M. Boone, L. Meuris, I. Lemmens, N. Van Roy, A. Soete, J. Reumers, M. Moisse, S. Plaisance, R. Drmanac, J. Chen, F. Speleman, D. Lambrechts, Y. Van de Peer, J. Tavernier and N. Callewaert, *Nat. Commun.*, 2014, **5**, 4767-4779.